metals

MDPI

Article

Effect of Nb on δ Phase Precipitation and the Tensile Properties in Cast Alloy IN625

Yiqiang Mu [1,2], Changshuai Wang [2], Wenlong Zhou [1] and Lanzhang Zhou [2,*]

1 School of Materials Science and Engineering, Dalian University of Technology, Dalian 116024, China; yqmou@imr.ac.cn (Y.M.); wlzhou@dlut.edu.cn (W.Z.)
2 Institute of Metal Research, Chinese Academy of Science, Shenyang 110016, China; cswang@imr.ac.cn
* Correspondence: lzz@imr.ac.cn; Tel.: +86-133-3244-9701

Received: 5 January 2018; Accepted: 18 January 2018; Published: 24 January 2018

Abstract: Cast alloy IN625 is a candidate Ni-base alloy for advanced ultra-supercritical (A-USC) power plants. The aim of this study was to investigate the influences of Nb on δ phase precipitation and the tensile properties in this alloy. The results show that the δ phase is easy to precipitate after long-term aging at 700 °C (the service temperature of A-USC power plants) and it is strongly affected by the content of Nb in the alloy. The strength of alloys after aging at 700 °C for 10,000 h increases with the increasing Nb content and also increases sharply when compared to that of as-heat-treated alloys. The increase in strength is found to be primarily associated with the precipitation of the δ phase.

Keywords: δ phase precipitation; element Nb; tensile properties; cast alloy IN625

1. Introduction

Advanced ultra-supercritical (A-USC) power plant is a term used to designate a coal-fired power plant design with a maximum steam temperature of 700 °C or above. Its goal is to reduce CO_2 emissions from coal-fired electric generating plants with improved thermal efficiency. As any type of martensitic advanced ferritic steel cannot meet the demand of A-USC power plants, high-strength Ni-base alloys are required. However, cast nickel-based superalloys, which possess high strength, creep resistance, and weldability, are typically not available, particularly those with good ductility and toughness that are weldable in thick sections [1]. To address those issues related to large castings in A-USC power plants, cast analogs of wrought nickel-based superalloy IN625 are selected as candidate materials for their good high strength, excellent fabricability, and outstanding corrosion resistance [1–8]. Although there are many studies in the literature on alloy IN625, most of the reports are about wrought alloy IN625 [7–22]. So, studies on cast alloy IN625, such as the one presented in this paper, is needed to investigate its potential application in A-USC power plants.

According the studies on wrought alloy IN625, the δ phase is observed to precipitate easily after long-term aging at 700–760 °C (the service temperature of A-USC power plants) [9–13], although it is initially designed as a solid solution hardening alloy [14]. The δ phase is an equilibrium phase corresponding to the γ'' phase with a composition of Ni_3Nb and an orthorhombic ($D0_a$) crystal structure [15–18]. The δ particles have needle, plate, as well as globular morphologies [19–22]. The normal form of the δ phase generally nucleates at grain boundaries, but at relatively high temperatures (850–900 °C) also forms in an intragranular fashion [19,23]. However, studies on the δ phase precipitation in cast alloy IN625 are scarce [24]. Moreover, increasing the Nb concentration is found to increase the driving force to form the δ phase [25], so it is excepted the fraction of the δ phase can be controlled by changing the Nb content. There is no available data about the effect of Nb on δ phase precipitation in cast alloy IN625. Considering the abovementioned information, this work aims to determine the effects of Nb on δ phase precipitation and the tensile properties in cast alloy IN625.

2. Materials and Methods

The nominal compositions of the experimental alloys used in this study are listed in Table 1. The alloy with a low Nb content cannot meet the strength requirement for A-USC power plants, while a high Nb content is bad for the processability of the alloy. Therefore, the Nb contents were chosen to be 3.15 wt. %, 3.8 wt. %, and 4.5 wt. %, respectively. The alloys were prepared by vacuum induction and then solution-treated at 1200 °C for 1 h followed by air cooling (AC). The high solution anneal used in this work is employed to develop the maximum softness for producing the large casting used in A-USC power plants. The alloys were aged at 700 °C for up to 10,000 h, with a primary aim of observing the δ precipitation after long-term aging at the service temperature of A-USC power plants.

Metallographic samples were prepared for observation in a JSM-6301F Scanning Electron Microscope (SEM, Jeol Instruments, Tokyo, Japan) equipped with energy dispersive spectroscopy (EDS, Oxford Instruments plc, Oxfordshire, UK) in the as-heat-treated and as-aged conditions. Confirmation of the identification of the phases was performed using a TECNAI G2 F30 transmission electron microscope (TEM, FEI, Hillsboro, AL, USA). Tensile tests at 700 °C were carried out on a Shimadzu AG-250KNE test machine (Shimadzu Corporation, Tokyo, Japan). The cylindrical, threaded tensile test rods with a gauge length of $\Phi 5$ mm × 25 mm machined from the thermally exposed bars were prepared as Standard GB/T 4338-2006 [26]. Each datum is an average of at least two tensile tested values.

Table 1. The nominal compositions of the experimental alloys (wt. %).

Alloy	Nb	Mo	Cr	C	Ni
3.15Nb	3.15	9	21.5	0.05	Bal.
3.8Nb	3.8	9	21.5	0.05	Bal.
4.5Nb	4.5	9	21.5	0.05	Bal.

3. Results and Discussion

3.1. Microstructure Evolution

The micrograph in Figure 1a shows the equiaxed structure of the experimental alloys as-cast. EDS-measured compositions (wt. %) at different positions and partition coefficients are summarized in Table 2. The segregation level of alloying elements in as-cast structures can be expressed by the partition coefficient between the interdendritic region and the dendrite core: $K = C_D/C_I$, where C_I and C_D are the concentration of the element in the interdendritic region and in the dendrite core, respectively. It is noteworthy that the content of Nb has a marked impact on the segregation level of Nb [27]. The segregation level of element Nb increases with the increasing Nb content. The general microstructures of the Nb series of alloys after solution-treatment are shown in Figure 1b. The materials are found to be rather free of any grain boundary or matrix precipitation, except for a few isolated blocky precipitates in the interdendritic region. EDS quantitative results (Figure 1d) of the phases show that it is enriched in Nb and C, which are believed to be primary carbides. At this condition, no δ phase is observed in the experimental alloys.

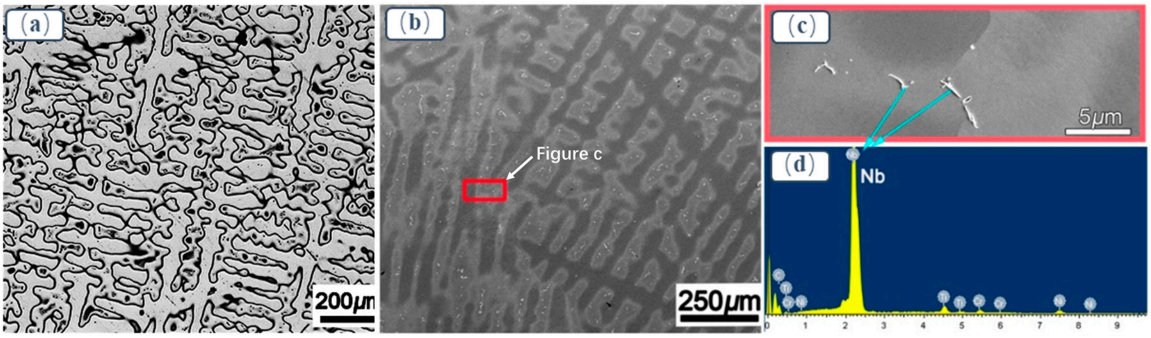

Figure 1. The structure of alloys as-cast (**a**), as-heat-treated (**b**), and EDS (energy dispersive spectroscopy) results of MC type carbide(NbC) (**c**,**d**).

Table 2. EDS results and calculated partition coefficients for as-cast IN625.

Alloy	3.15Nb				3.8Nb				4.5Nb			
Element	Nb	Mo	Cr	Ni	Nb	Mo	Cr	Ni	Nb	Mo	Cr	Ni
C_D, wt. %	1.8	8.5	22.9	66.9	1.9	7.5	23.0	67.6	1.9	7.5	23.0	66.9
C_I, wt. %	5.1	9.9	20.8	64.2	5.8	10.1	21.0	63.1	7.2	10.2	20.3	62.3
K	2.83	1.16	0.91	0.96	3.05	1.34	0.91	0.93	3.60	1.31	0.87	0.93

The micrographs in Figures 2 and 3 show the microstructures of the 3.15Nb, 3.8Nb, and 4.5Nb alloys after aging at 700 °C for 500 h and 3000 h. Following aging for 500 h, a few small δ phase precipitates are observed along NbC carbides (Figure 2b,c) and the grain boundaries (Figure 2d) in the 3.8Nb and 4.5Nb alloys, while no δ phase precipitates are found in the 3.15Nb alloy (Figure 2a). This suggests that a greater addition of Nb can promote the precipitation of the δ phase. The initial precipitation positions of the δ phase are believed to be along the grain boundaries and NbC carbides, which are further verified by the microstructures of 3.15Nb, 3.8Nb, and 4.5Nb alloys aged for 3000 h (Figure 3). Identification of the δ phase is based on the TEM and the EDS results presented in Figure 4.

The micrographs in Figure 5 show the microstructures of the 3.15Nb, 3.8Nb, and 4.5Nb alloys aged at 700 °C for 5000 h and 10,000 h. Prolonged aging of the experimental alloys at 700 °C resulted in a significant increase in volume fraction of the δ phase precipitates for all of the Nb series of alloys. The increasing fraction of the δ phase precipitates corresponds to increases in the overall Nb content. In order to provide a visualized description of the relations between the addition of Nb content and the δ precipitation in the experimental alloys, the volume fraction of the δ precipitate is measured using Image-Pro Plus 6.0 software (Media Cybernetics Inc., Rockville, MD, USA) from the scanning electron microscope (SEM, Jeol Instruments, Tokyo, Japan) micrographs. Considering that the δ precipitates in the alloy are mostly concentrated in the interdendritic regions due to the segregation of Nb (as shown in Figure 6), it may provide accurate statistics if the magnification of the micrographs is small enough and appropriate to clearly detect the δ precipitates for analysis. The results are plotted as a function of aging time and Nb content (Figure 7). The volume fraction of the δ precipitation increases with both the aging time and Nb content. The effect of Nb content on the fraction of the δ phase corresponds to its effect on the Nb segregation degree. The more seriously the element Nb segregates, the more Nb can segregate at excess vacancies, dislocations, and extrinsic stacking faults in the γ matrix [14]. This results in the reduction of the critical nucleus free energy, and further promotes the precipitation of the δ phase.

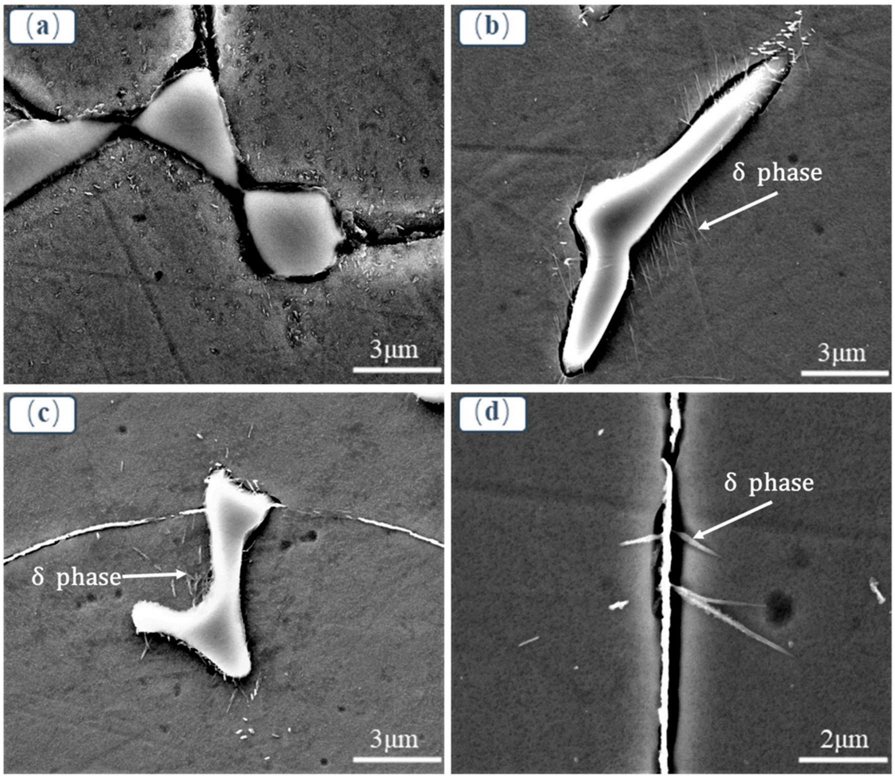

Figure 2. The precipitation of the δ phase along NbC carbides in alloy 3.15Nb (**a**), 3.8Nb (**b**), and 4.5Nb (**c**), and the grain boundaries in alloy 4.5Nb (**d**) after aging at 700 °C for 500 h.

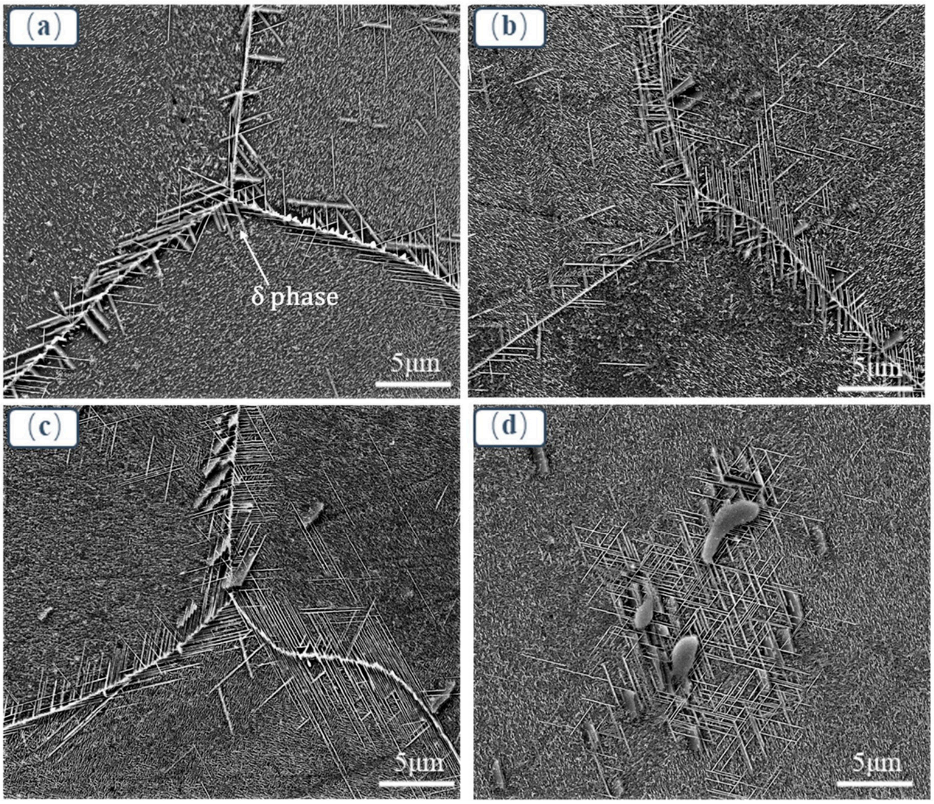

Figure 3. SEM micrographs of the δ phases along the grain boundaries for aging at 700 °C for 3000 h in alloy 3.15Nb (**a**), 3.8Nb (**b**), and 4.5Nb (**c**), and NbC carbides in the Nb series of alloys (**d**).

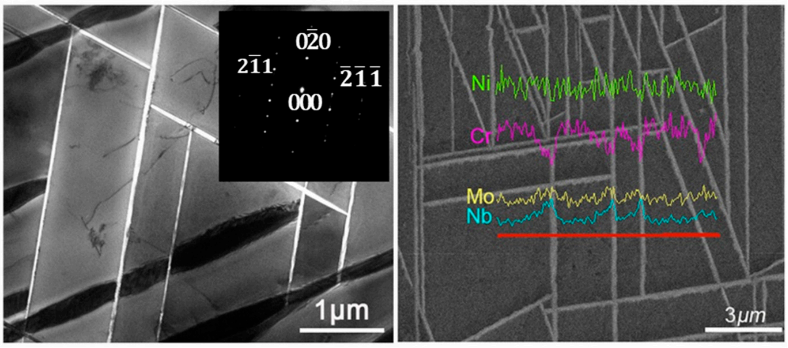

Figure 4. Identification of the δ phases based on TEM and the EDS results.

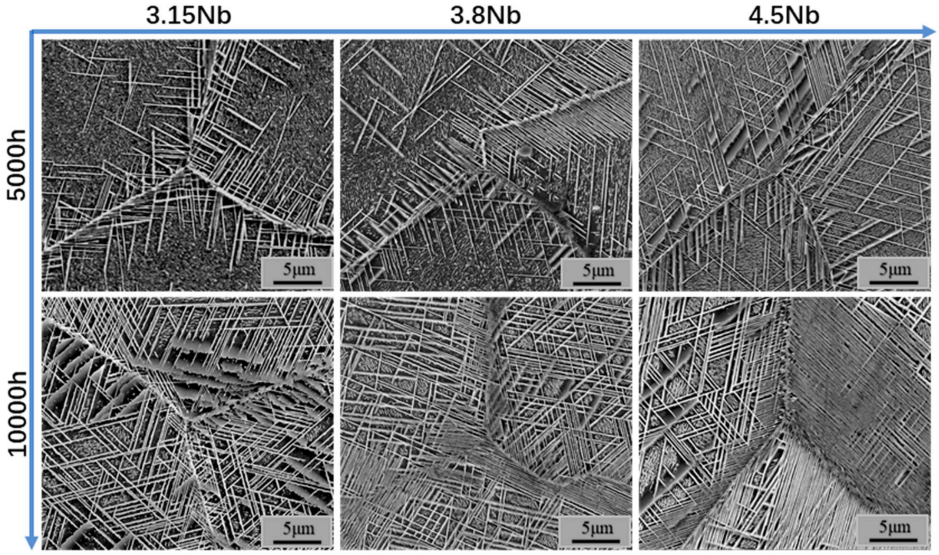

Figure 5. SEM micrographs of the δ phases along grain boundaries in the Nb series of alloys after aging at 700 °C for 5000 h and 10,000 h.

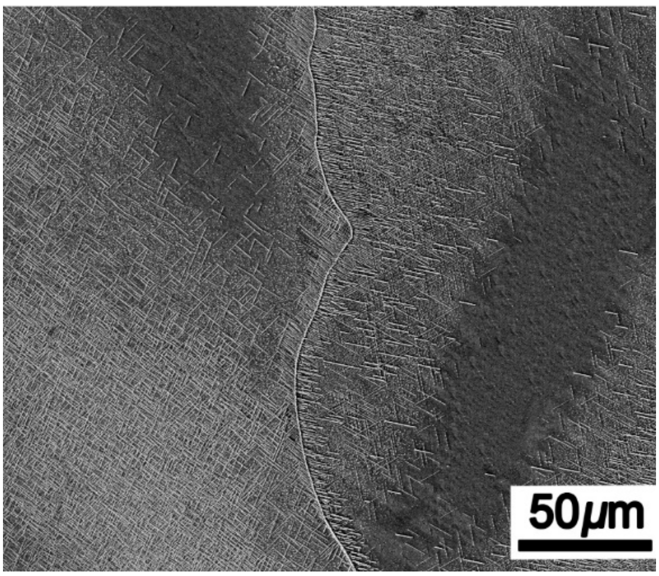

Figure 6. SEM micrographs of the δ phases precipitation in alloy 3.15Nb aged for 10,000 h.

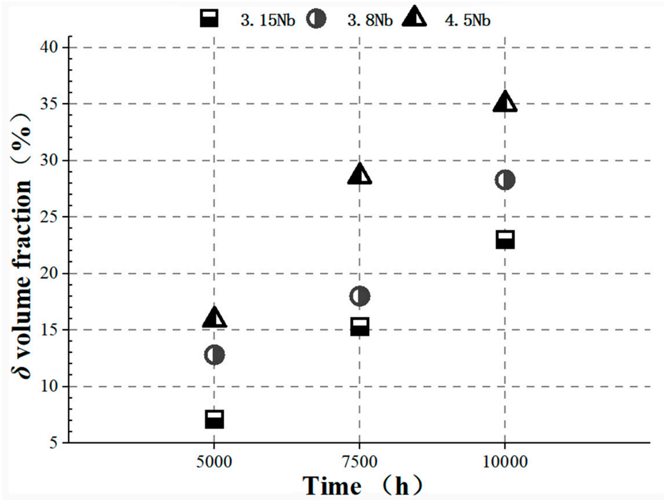

Figure 7. δ phase volume fraction evolution as a function of aging time and Nb content.

3.2. Tensile Properties

A substantial precipitation of the δ phases in the experimental alloys after long-term aging at 700 °C suggests that the critical applications of the alloy need further investigation to elucidate its role in affecting tensile properties. The tensile properties of alloys as-heat-treated and aged at 700 °C for 10,000 h are both presented in Table 3. The yield strength (YS), ultimate tensile strength (UTS), and elongation (EL) after solution treatment are around 180 MPa, 400 MPa, and 50%, respectively. The tensile properties are comparable among the different specimens; no obvious change in the tensile properties of the as-heat-treated alloys with varied additions of Nb is noticed. Meanwhile, for the alloy treated with prolonged aging at 700 °C for 10,000 h, the yield strength and ultimate tensile strength at 700 °C are sharply increased. At this given condition, the tensile properties also vary strongly with the Nb content. The aging of the alloys also leads to a decrease in ductility. It is worth noting that the Nb content has little effect on the value of EL under the same given conditions.

Table 3. The tensile properties of alloys as-heat-treated and aged at 700 °C for 10,000 h.

Condition	As-Heat-Treated			Aged at 700 °C for 10,000 h		
Alloy	**3.15Nb**	**3.8Nb**	**4.5Nb**	**3.15Nb**	**3.8Nb**	**4.5Nb**
YS	175	180	175	595	650	710
UTS	420	410	385	720	780	880
EL	62	50	63	9	13	8

It is interesting to find that the effects of Nb content on the tensile properties are totally different between the as-heat-treated alloys and those aged at 700 °C for 10,000 h. For the as-heat-treated alloys, the effect of Nb content on the strength of the alloys is not obvious. However, after aging at 700 °C for 10,000 h, the strength is strongly affected by the Nb content. Considering that the major change of microstructure is the δ phase precipitation and its fraction increases with the increasing Nb content, the strength increase with Nb content after aging is believed to be closely related to the δ precipitates. To confirm this deduction, the dislocation substructure of alloys was observed under TEM. Figure 8a shows an example of the dislocation substructure of as-heat-treated alloys. It is seen that tangled jogged dislocations are associated with cross slip (the transfer of a screw dislocation from one {111} system to another {111}, whereas straight uniformly distributed dislocations reflect more difficult cross slip [28]. The dislocation substructure of alloys after aging for 10,000 h, by contrast, changed completely due to the δ phase precipitation. As shown in Figure 8b, the tangles have straightened-out considerably and some interaction to form three or more-fold nodes has taken place. The high-density tangled dislocations pinned by the δ phase precipitate results in the stress concentration around the δ phase when the motion of dislocation is prevented. This should provide the potential for improving strength [29]. It is believed that the δ precipitates serve as a strengthening phase in the experiment alloy. If the effect of Nb on the fraction of the δ phase is taken into account at the same time, it is determined that the different role of Nb in the strength of the as-heat-treated alloy and the alloy aged at 700 °C for 10,000 h is primarily associated with the precipitation of the δ phase.

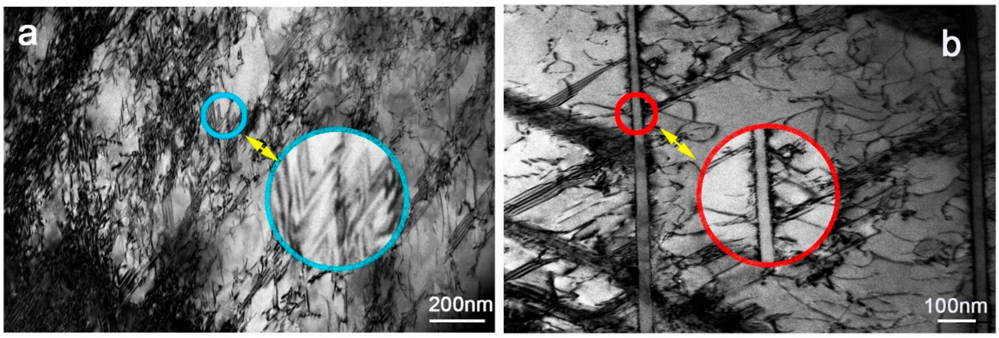

Figure 8. The dislocation substructure of alloys as-heat-treated (**a**) and aged for 10,000 h (**b**) after tensile tests.

Figure 9 shows SEM micrographs of the tensile fracture surface of the alloy as-heat-treated and as-aged for 10,000 h. The fracture surfaces are observed along the interdendritic region, because it is the weakest area in the cast alloys. The fracture features reveal that the δ phase has an effect on fracture morphology, being more brittle with the precipitation of the δ phase. It is worth mentioning that the varied fraction of the δ phase (for the alloys aged for 10,000 h) has a small effect on the value of elongation.

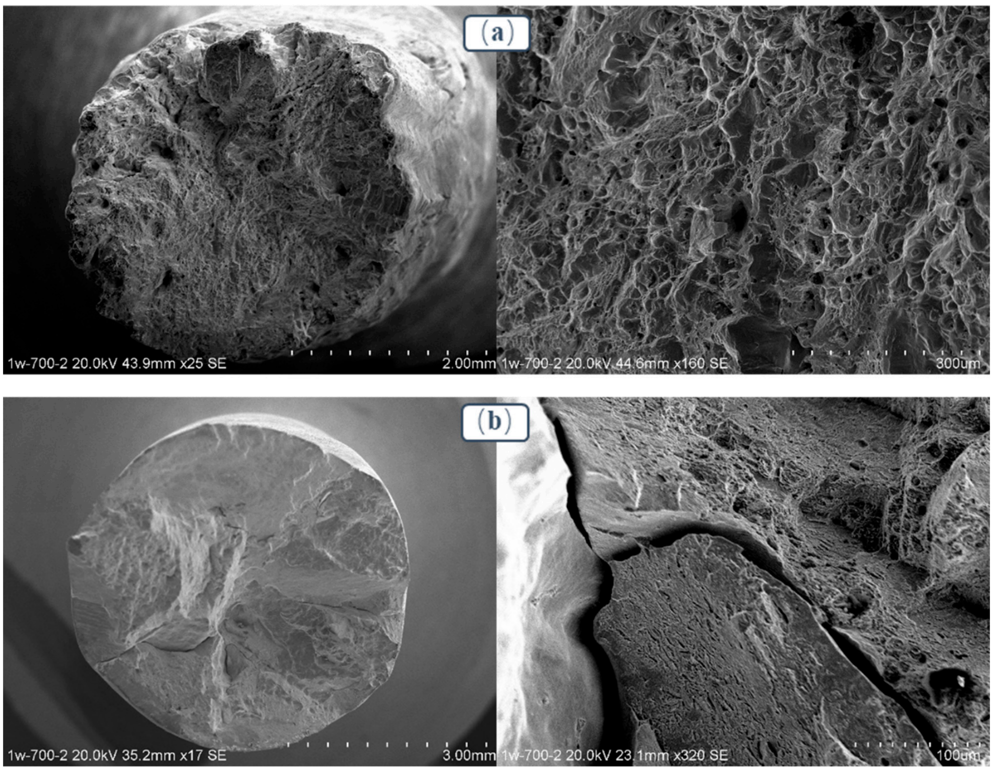

Figure 9. Fracture surfaces of the alloy 4.5Nb as-heat-treated (**a**) and as-aged for 10,000 h (**b**).

4. Conclusions

The effects of Nb on δ phase precipitation and the tensile properties in cast IN625 are investigated in this paper. It is found that increasing the Nb content promotes the precipitation of the δ phase due to the increasing Nb segregation. The effect of Nb on tensile properties is divided into two different situations. One is that the effect is not obvious for the as-heat-treated alloys. Another is that the effect is strong for the alloys aged at 700 °C for 10,000 h, which is primarily associated with the precipitation of the δ phase. δ precipitation is believed to serve as a strengthening phase in cast alloy IN625.

Acknowledgments: This work was financially supported by the National Energy Administration Program of China (No. NY20150102), the National Key Research and Development Program of China (No. 2017YFB0305204) and the National Natural Science Foundation of China (No. 51571191).

Author Contributions: Lanzhang Zhou and Wenlong Zhou conceived and designed the experiments; Yiqiang Mu and Changshuai Wang performed the experiments; Yiqiang Mu and Changshuai Wang analyzed the data; Lanzhang Zhou contributed reagents/materials/analysis tools; Yiqiang Mu wrote the paper.

Conflicts of Interest: The authors declare no conflict of interest. The founding sponsors had no role in the design of the study; in the collection, analyses, or interpretation of data; in the writing of the manuscript, and in the decision to publish the results.

References

1. Jablonski, P.D.; Hawk, J.A.; Cowen, C.J.; Maziasz, P.J. Processing of advanced cast alloys for A-USC steam turbine applications. *JOM* **2012**, *64*, 271–279. [CrossRef]
2. Nair, A.; Kumanan, S. Newer Materials for Supercritical Power Plant Components—A Manufacturability Study. In Proceedings of the International Conference on Advances in Production and Industrial Engineering, Tiruchirappalli, India, 20–21 February 2015; pp. 326–332.
3. De Albuquerque, V.H.C.; Barbosa, C.V.; Silva, C.C.; Moura, E.P.; Filho, P.P.R.; Papa, J.P.; Tavares, J.M.R.S. Ultrasonic Sensor Signals and Optimum Path Forest Classifier for the Microstructural Characterization of Thermally-Aged Inconel 625 Alloy. *Sensors* **2015**, *15*, 12474–12497. [CrossRef] [PubMed]
4. Abe, F. Research and Development of Heat-Resistant Materials for Advanced USC Power Plants with Steam Temperatures of 700 °C and Above. *Engineering* **2015**, *1*, 211–224. [CrossRef]
5. Lückemeyer, N.; Kirchner, H.; Almstedt, H. Challenges in Advanced-USC Steam Turbine Design for 1300°F/700°C, GT2012-69822. In Proceedings of the ASME Turbo Expo 2012: Turbine Technical Conference and Exposition, Copenhagen, Denmark, 11–15 June 2012.
6. Siefert, J.A.; Shingledecker, J.P.; DuPont, J.N.; David, S.A. Weldability and weld performance of candidate nickel based superalloys for advanced ultrasupercritical fossil power plants Part II: Weldability and cross-weld creep performance. *Sci. Technol. Weld. Join.* **2016**, *21*, 397–427. [CrossRef]
7. Castello, D.; Rolli, B.; Kruse, A.; Fiori, L. Supercritical Water Gasification of Biomass in a Ceramic Reactor: Long-Time Batch Experiments. *Energies* **2017**, *10*, 1734. [CrossRef]
8. Cárcel-Carrasco, F.-J.; Pérez-Puig, M.-A.; Pascual-Guillamón, M.; Pascual-Martinez, R. An Analysis of the Weldability of Ductile Cast Iron Using Inconel 625 for the Root Weld and Electrodes Coated in 97.6% Nickel for the Filler Welds. *Metals* **2016**, *6*, 283. [CrossRef]
9. Floreen, S.; Fuchs, G.E.; Yang, W.J. The metallurgy of alloy 625. In *Superalloys 718, 625 and Various Derivatives*; TMS-AIME: Warrendale, PA, USA, 1991; pp. 13–37.
10. Moore, I.J.; Taylor, J.I.; Tracy, M.W.; Burke, M.G.; Palmiere, E.J. Grain coarsening behaviour of solution annealed Alloy 625 between 600–800 °C. *Mater. Sci. Eng. A* **2017**, *682*, 402–409. [CrossRef]
11. Suave, L.M.; Bertheau, D.; Cormier, J.; Villechaise, P.; Soula, A.; Hervier, Z.; Laigo, J. Impact of microstructural evolutions during thermal aging of Alloy 625 on its monotonic mechanical properties. In Proceedings of the MATEC Web of Conferences, Giens, France, 12–16 May 2014; p. 21001.
12. Lass, E.A.; Stoudt, M.R.; Williams, M.E.; Katz, M.B.; Levine, L.E.; Phan, T.Q.; Gnaeupel-Herold, T.H.; Ng, D.S. Formation of the Ni3Nb/delta-Phase in Stress-Relieved Inconel 625 Produced via Laser Powder-Bed Fusion Additive Manufacturing. *Metall. Mater. Trans. A* **2017**, *48*, 5547–5558. [CrossRef]

13. Suave, L.M.; Cormier, J.; Villechaise, P.; Soula, A.; Hervier, Z.; Bertheau, D.; Laigo, J. Microstructural evolutions during thermal aging of alloy 625: Impact of temperature and forming process. *Metall. Mater. Trans. A* **2014**, *45*, 2963–2982. [CrossRef]
14. Eiselstein, H.L.; Tillack, D.J. The invention and definition of alloy 625. In *Superalloys 718, 625 and Various Derivatives*; TMS-AIME: Warrendale, PA, USA, 1991; pp. 1–14.
15. Mathew, M.D.; Bhanu Sankara Rao, K.; Mannan, S.L. Creep properties of service-exposed Alloy 625 after re-solution annealing treatment. *Mater. Sci. Eng. A* **2004**, *372*, 327–333. [CrossRef]
16. Kim, J.-S.; Lee, H.-W. A Study on Effect of Intergranular Corrosion by Heat Input on Inconel 625 Overlay Weld Metal. *Int. J. Electrochem. Sci.* **2015**, *10*, 6454–6464.
17. Malej, S.; Medved, J.; Batič, B.Š.; Tehovnik, F.; Godec, M. Microstructural evolution of Inconel 625 during thermal aging. *Metalurgija* **2017**, *56*, 319–322.
18. Di, X.J.; Xing, X.X.; Wang, B.S. Nucleation and Coarsening Mechanism of Δ Phase in Inconel 625 Deposited Metal. *Acta Metall. Sin.* **2014**, *50*, 323–328.
19. Sundararaman, M.; Mukhopadhyay, P.; Banerjee, S. Precipitation of the delta-Ni3Nb phase in two nickel base superalloys. *Metall. Trans. A* **1988**, *19*, 453–465. [CrossRef]
20. Muzyka, D.R.; Maniar, G.N. Effects of solution treating temperature and microstructure on the properties of hot-rolled 718 alloy. *Met. Eng. Q* **1969**, *9*, 23–37.
21. Zhu, Z.Y.; Sui, Y.; Dai, A.L.; Cai, Y.F.; Xu, L.L.; Wang, Z.X.; Chen, H.M.; Shao, X.M.; Liu, W. Long term aging treatment impact on ultralow iron Alloy 625 intergranular corrosion property. *Preprints* **2017**. [CrossRef]
22. Ding, Y.T.; Gao, Y.B.; Dou, Z.Y.; Gao, X.; Liu, D.X.; Jia, Z. Precipitation Behavior of delta Phase of Deformation Induced GH3625 Superalloy Hot-Extruded Tube. *Acta Metall. Sin.* **2017**, *53*, 695–702.
23. Kirman, I. Precipitation in the Fe-Ni-Cr-Nb system. *J. Iron Steel Inst.* **1969**, *207*, 1612–1618.
24. Singh, J.B.; Verma, A.; Jaiswal, D.M.; Kumar, N.; Patel, R.D.; Chakravartty, J.K. Rejuvenation of service exposed ammonia cracker tubes of cast Alloy 625 and their re-use. *Mater. Sci. Eng. A* **2015**, *644*, 254–267. [CrossRef]
25. Singh, J.B.; Sundararaman, M.; Mukhopadhyay, P.; Prabhu, N. Effect of ternary Nb additions on the stability of the $D0_{22}$ structure of the Ni_3V phase. *Scr. Mater.* **2003**, *48*, 261–267. [CrossRef]
26. International Organization for Standardization. *Metallic Materials—Tensile Testing at Elevated Temperature (ISO 783: 1999, MOD)*; GB/T4338-2006; International Organization for Standardization: Geneva, Switzerland, 1999; p. 5.
27. Gao, G.; Zhang, M.; Dong, J.; Yao, Z.; Zheng, L. Effects of Nb Content Variations on Precipitates Evolution of GH4169 Ingots during Their Solidification and Homogenization Processes. *Rare Met. Mater. Eng.* **2014**, *43*, 103–108.
28. McEvily, A.J.; Johnston, T.L. The role of cross-slip in brittle fracture and fatigue. *Int. J. Fract. Mech.* **1967**, *3*, 45–74. [CrossRef]
29. McLaren, A.C.; Retchford, J.A. Transmission electron microscope study of the dislocations in plastically deformed synthetic quartz. *Phys. Stat. Solidi* **1969**, *33*, 657–668. [CrossRef]